Risk Mitigation Approaches for Improved Resilience in Distribution Networks

Jonatas Boas Leite[1], *Member*, *IEEE*
[1]*Dep. of Electrical Engineering*
São Paulo State University - UNESP
Ilha Solteira - SP, Brasil
jb.leite@unesp.br

Mladen Kezunovic[2], Life *Fellow*, *IEEE*
[2]*Dep. of Electrical and Computer Engineering*
Texas A&M University
College Station - TX, USA
kezunov@ece.tamu.edu

***Abstract*— traditionally the risk analysis framework comprises two steps: risk assessment and risk mitigation. The tracking of operating conditions for each feeder section of a distribution network using the prediction of hourly risk levels and monthly accumulated risks corresponds to the first step. In this paper, we evaluate the use of two modern approaches to risk mitigation, one commonly named as automatic fault location, isolation and service restoration (FLISR), and other as demand response management (DRM). Since the implementation of these approaches depends on distribution automation, the control actions to mitigate the risk are carried out through the distribution management system. Results reveal advantages in the implementation of FLISR and DRM for improving the distribution network resilience. The developed visualization tool with georeferenced data from a real-world distribution network supports the achieved benefits.**

Keywords-- Power Distribution System, Resilience, Predictive Risk Assessment, Risk Mitigation, Fault Location, Isolation and Service Restoration (FLISR), Demand Response Management (DRM).

I. INTRODUCTION

The risk control can prevent failures and mitigate consequences through the definition of acceptable risk and comparative evaluation of feasible choices based on monitoring and decision analysis. A key for affective ranking of risk reduction measures and proactive risk management employs risk-based technologies [1]. The correlation between historical management data of power distribution systems and available weather data supports the risk measurement for weather-based risk assessment. Predicted risk levels aid to determinate the power distribution network state in cooperation with some method of power system security analysis that continuously monitors the operating condition.

As operating conditions vary throughout the day, the power system must be maintained in normal secure state. In a normal secure state, there is energy supply to all loads and no operating limit is exceeded [2] while, in a normal insecure state, the power balance in each bus and all operating inequality constraints also remain satisfied, but the power system is vulnerable to some contingencies [3]. Since any permanent fault in the power distribution system causes load losses, the assertion that distribution networks operate in normal insecure state is legitimate, consequently, the identification of feeder sections with high risk level is a strong indication of alert state requiring preventive actions to mitigate impacts of an energy supply interruption.

In the risk-based decision-making framework [4], the correlation between likelihood and impact describes the risk assessment, i.e. the risk is assessed as the likelihood that hazards will unfold to explore vulnerabilities to provoke impacts on specific targets [5]. When the high-risk level is identified, load balancing allows dynamic reallocation of loads to adjacent feeders [6], and automatic restoration optimization provides adjustment parameters of adaptive protection devices [7] to ensure the power transfer. The feasibility of these control actions comes from self-healing technologies that include automatic fault location, isolation and service restoration (FLISR) and demand response management (DRM).

As it is very expensive and rather unrealistic to replace, upgrade or make all components of the power system more robust [8], risk analysis provides a powerful methodology capable of assisting in control actions. The consequent benefits include the improved resilience in distribution networks where unfavorable events are anticipated, mitigation strategies are determined and the power grid is rapidly adapted and restored, as described in [9]. Our contribution in this paper is the integration of two self-healing technologies, automatic FLISR and DRM, into a risk mitigation approach. After the resilience improvement, the reexamination of distribution network is made using a developed visualization tool based on the geographical information system (GIS) that assigns different colors to each level of risk in the graphical representation of feeder sections.

II. PREDICTIVE RISK ASSESSMENT FRAMEWORK

The correlation between the likelihood of an event occurring over time and its consequent impacts provides a measurement of risk [4]. The computation of the failure probability for each feeder section uses (1) and (2). The observed statuses of features of interest, x_i, composes the vector of current external dependences $\boldsymbol{X}=\{x_i|dom(x_i)=dom(f)=\{0,1\} \wedge i=1,...,D\}$, where D is the number of features of interest. The analyzed data comes from external servers for lightning monitoring and weather forecasting as well as vulnerability models for vegetation growth and aging degradation of power system components.

The São Paulo Research Foundation – FAPESP (grant: 2019/07436-5) has been fully supported this work.

$$p(f \mid \boldsymbol{X}) = \frac{\tilde{p}(\boldsymbol{X} \mid f)\tilde{p}(f)}{\sum_f \tilde{p}(\boldsymbol{X} \mid f)\tilde{p}(f)} \quad (1)$$

$$\tilde{p}(\boldsymbol{X} \mid f) = \prod_{i=1}^{D} (\tilde{\theta}^{f}_{i,m,y+1})^{x_i} (1 - \tilde{\theta}^{f}_{i,m,y+1})^{1-x_i} \quad (2)$$

where

$p(f|\boldsymbol{X})$: Conditional probability of failure subject to $\boldsymbol{X}$;
$\tilde{p}(\boldsymbol{X}|f)$: Estimate of the likelihood of $\boldsymbol{X}$ given f;
$\tilde{p}(f)$: Estimate of failure probability;
$\tilde{\theta}^{f}_{i,m,y+1}$: Estimate of the probability of observing x_i conditioned to a failure event f in the current m-th month of the current year.

The calculation of energy supply interruption cost with georeferenced network data of fault event locations and interruption cost formulation based on time series provides the impact quantification as in [5] and [10]. The various stakeholders in the energy market, such as utility company, regulatory authority and energy consumers, perceive different costs and their sum yields the total cost of power interruption, C^{TOTAL}, as is given in (3).

$$C^{\mathrm{TOTAL}} \sim \sum_{i\in\boldsymbol{\Omega}} \sum_{j\in\boldsymbol{\Phi}} \left(\left((1+H_i)c^{e}_{j} + c^{CDF}_{i}\right) L_j \sum_{m\in\boldsymbol{\Theta}} \sum_{n\in\boldsymbol{T}} F^{dem}_{i,m,n} w_{j,m,n} \right) z_{i,j} \quad (3)$$

where

$\boldsymbol{\Omega}, \boldsymbol{\Phi}$, $\boldsymbol{\Theta}, \boldsymbol{T}$: Set of time series, all customers on the feeder, most typical customer types and consumption profiles;
H_i : Billing loss penalty function;
c^{e}_{j} : Electricity rate;
c^{CDF}_{i} : Customer damage function;
L_j : Installed power;
$F^{dem}_{i,m,n}$: Load percentage demand hour-by-hour;
$w_{j,m,n}$: Type and consumption profile of the j-th customer;
$z_{i,j}$: Interruption state changes of the j-th customer.

The matrix, which ranks the risk in levels through a classification method, provides the correlation between $p(f|\boldsymbol{X})$ and C^{TOTAL}. Elements of this matrix are grouped in three levels: unacceptable risk as the high level (H); undesirable and acceptable risk with review as the medium level (M); and acceptable risk as the low level (L).

III. Risk Mitigation with FLISR and DRM

The key issue in any risk analysis approach is the anticipation of damages in order to take proactive risk mitigation strategies [11]. Instead of merely responding to the last event, a risk-based decision-making framework allows for setting priorities under common constraints of time and money. In this way, the coordination of automatic FLISR with DRM can release power capacity that is needed to restore consumption areas reducing interruption time and cost.

A. Interruption Time Reduction using Automatic FLISR

The capabilities of distribution automation are important factors in the implementation of FLISR schemes allowing adaptive protection by controlling relay settings in real-time [12]. A benefit of implementing FLISR is the substantial reduction in power interruption time and improved system reliability [13]. Without FLISR, several steps need to be taken, such as outage report, travel to the site, fault investigation and patrol, before the fault is isolated and adjacent un-faulted sections are restored by manual switching [14]. FLISR schemes automate the fault location, isolation of the faulted section, and service restoration of un-faulted adjacent sections, minimizing the restoration time of faulted section while preserving the energy supply for consumers at adjacent un-faulted sections [15]. In a power distribution system with FLISR, the adjacent un-faulted sections are restored in a short time, but the faulted section still requires travel, patrol and repair time intervals. Furthermore, the use of adaptive protection reduces power supply interruption on unaffected sections [16].

In the context of risk assessment, the understanding of interruption time is fundamental to mitigate the financial impact. Since the operating state of energy consumers can be changed by fault management procedures, in (3) the binary variable $z_{i,j}$ reflects the interruption of power supply to the j-th consumer during the fault event.

$$z_{i,j} = \begin{cases} 1 & i\partial t \le \Delta t_j \\ 0 & otherwise \end{cases} \quad \forall i \in \boldsymbol{\Omega} = \left\{1,2,\ldots \left\lceil \frac{\Delta t}{\partial t} \right\rceil \right\}, \forall j \in \boldsymbol{\Phi} \quad (4)$$

The interruption time needed to repair and restore the faulted section, Δt, is discretized by a pre-defined time-step, ∂t, yielding the set of time series $\boldsymbol{\Omega}$. Thus, in (4), Δt_j comprises the time interval in which the j-th consumer does not have energy supply from the power grid.

B. Interruption Cost Mitigation using DRM

Traditionally, the power generation matches the load demand, reserve margin for peak demand and reserve energy during contingences. As power supply constraints persist, power distribution technologies, like distributed generation (DG) and demand response (DR) programs, have received great attention for cost reduction and capacity relief [17]. DRM can aid the consumer through the efficient use of energy using remote monitoring and controlling loads and suitably pricing the energy to reduce the demand on peak hours [18].

Although most literature focuses on pricing strategies to shift the high power demand to off-peak hours, the DR definition from the Federal Energy Regulatory Commission report also includes resilience issues by providing financial incentives to preserve the operating state of distribution networks [19], as following: "*Changes in electric use by demand-side resources from their normal consumption patterns in response to changes in the price of electricity, or to incentive payments designed to induce lower electricity use at times of high wholesale market prices or when system reliability is jeopardized*".

The demand-side resilience is the main concern in [20] where Hirohisa Aki reports the damage caused by Great East Japan Earthquake in 2011 and presents some learned lessons such as the importance of including broad responses against risks and the necessity of flexible business practices to manage

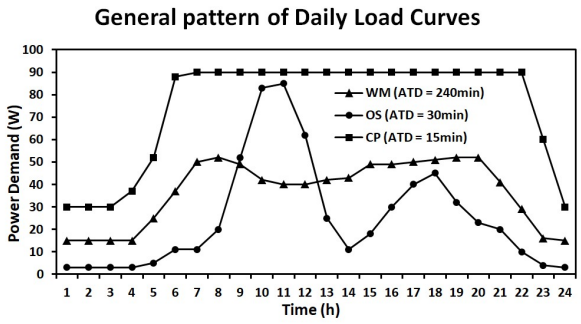

(a)

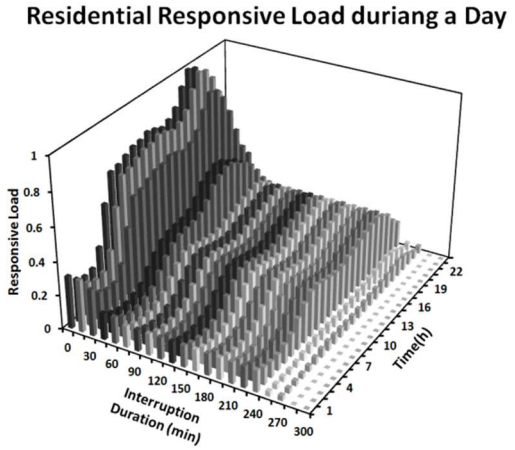

(b)

Fig. 1. Determination of changes in responsive load during the interruption time: (a) general pattern of load curves; and (b) residential responsive load.

these risks. His conclusion also highlights the DR program as a byproduct of the experienced power shortage with its recognition resulting in the initiation of "negawatt" market [21].

Figure 1 illustrates the behavior of the responsive load to residential consumers during a day that is achieved using the general pattern of daily load curves from appliances in residences. In Fig. 1 (a), the load curves of washing machine (WM), oven/stove (OS) and heating circulating pump (CP) reveal the differences in power demand patterns [23]. In addition to load curves of all residential appliances that can response to DR controller, acceptable time delay (ATD) values are required in the construction of the daily residential responsive load. Figure 1 (b) is achieved by the sum of hourly power demand of all residential appliances while their ATD values remain less than interruption duration. In residential consumers, the penetration of responsive load is larger than 50% of total power demand [22]. The procedure to achieve the responsive load of commercial and industrial consumers is similar to residential consumer but the penetration is different. In [18], for example, the DR controller actuates to shed the load when the instantaneous demand exceeds 90% of the contracted capacity or demand limit. In industry the shedding operation is more restrict due to production needs, but the use energy generation and storage can contribute to the responsive load penetration.

The responsive load represents the demand surplus and its control should straightforwardly affect the total cost of the power interruption, i.e. in the risk assessment framework the shedding of responsive loads mitigates the risk by reducing the financial impact. In the predictive risk assessment framework, the total cost, C^{TOTAL}, is formulated as in (3). The sum of costs related to different stakeholders in the energy market comprising the billing loss to utility company, $c_j^e L_j$, the penalty cost from regulatory authority rules, $H_i c_j^e L_j$, and the economic losses of residential, commercial and industrial consumers, $c_i^{CDF} L_j$. These three costs depend on total percentage of load demand, $F_{i,m,n}^{dem}$, that includes the demand surplus. Thus, the power demand with DRM, $F_{i,m,n}^{DRM}$, responds to shedding signal from DR controller when the distribution system is jeopardized.

$$F_{i,m,n}^{DRM} = F_{i,m,n}^{dem}(1-\delta_m F_{i,m}^{RL}) \;\forall i \in \boldsymbol{\Omega}, \forall m \in \boldsymbol{\Theta}, \forall n \in \boldsymbol{T} \quad (5)$$

In (5), the variable δ_m is the penetration percentage of responsive load for m-th type of consumer and $F_{i,m}^{RL}$ is the percentage of responsive load for m-th type of consumer during i-th time-step. In the case of residential consumer, the responsive load behaves as in Fig. 1 (b) where the maximum magnitude for each hour is at the beginning of the interruption period when the percentage responsive load is equal to one ($F_{0,0}^{RL}$=1.0). For commercial consumers, the arriving of electrical vehicles (EVs) during working hours pushes the percentage of responsive load to values above 1.0 as the energy generation during solar light hours for industrial consumers.

IV. Risk Assessment with Improved Resilience

In this section, the aforementioned advantages from the integration of smart grid technologies, such as automatic FLISR and DRM, are measured using the developed GIS visualization tool. This makes it possible to evaluate the functionality of the proposed application and analyze the use of smart grid technologies to mitigate the financial impact of energy supply interruption. In order to ensure the applicability of the GIS visualization tool, the test distribution network is a real-world feeder with ten sectionalizing switches limiting nine feeder sections with data available in [24]. The computation of quantified values of likelihood and impact for each feeder section is classified as in Table 1.

TABLE 1. Risk Matrix with Likelihood and Impact Categories.

			IMPACT (10^3)					
	Description	-	*Insigni-ficant*	*Minor*	*Signifi-cant*	*Serious*	*Major*	*Catastro-phic*
	-	Range	0.8-5.0	5.0-8.5	8.5-13.2	13.2-20.5	20.5-31.7	31.7-49.0
LIKELIHOOD	*Extremely Unlikely*	0.00-0.10	L	L	L	L	L	L
	Highly Unlikely	0.10-0.31	L	L	L	L	L	M
	Doubtful	0.31-0.54	L	L	M	M	M	H
	Very Unlikely	0.54-0.75	L	M	M	M	H	H
	Unlikely	0.75-0.91	M	M	M	H	H	H
	Likely	0.91-1.00	M	M	M	H	H	H

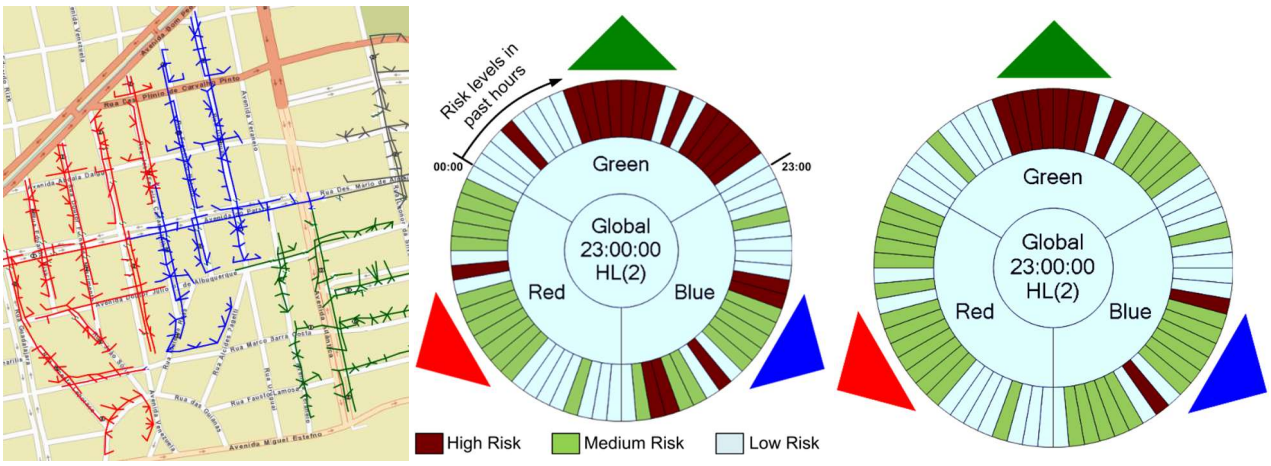

(a) (b) (c)

Fig. 2. Screenshots with (a) clusterized feeder and hourly sunburst chart to (b) base case and (c) distribution network with FLISR.

The evaluation of proposed risk mitigation technologies, i.e. the reexamination of risk level in each feeder section is done in two steps. In the first, expected improvements in the implementation of automatic FLISR in the test distribution network is measured using the hour-by-hour risk assessment and their results are compared with the base case. After that, monthly-accumulated risk magnitudes are achieved and compared, as well. In the second step, exactly the same evaluation approach is performed, but now, the risk mitigation technology comprises the implementation of both automatic FLISR and DRM.

The first step requires the specification of interruption time intervals. In adjacent un-faulted sections, the restoration of energy supply service took few minutes (from 1 to 5), while faulted sections inspection needs more time for field crew travel and device damage repair. Screenshots of the GIS visualization tool developed with sunburst chart approach [25] provide the result of the hourly risk assessment. Figure 2(a) shows a screen portion with feeder representation in three clusters: red, blue, and green. In the hourly risk levels for all analyzed cases, the light blue color corresponds to the low risk level, the olive green to medium and dark red to the high-risk level. The external cycle maintains the chronology of risk levels per cluster over the twenty-four hours daily by starting at zero hour (00:00). Comparatively, Fig 2 (b) displays the measured risk levels in the risk assessment for the base case, while the Fig. 2 (c) shows the same sunburst chart in which the screenshot is taken in the case where the test distribution network has automatic FLISR.

The red cluster of the feeder in the base case has a high level only at the 16:00. After the implementation of automatic FLISR, the hourly risk assessment pattern changes and becomes predominant with medium risk. The change is consequence of the financial impact reduction to *Insignificant* classification during whole day. The blue cluster of the feeder remains with medium risk predominance even after the FLISR implementation but the high-risk level, from 20:00 to 21:00, reduces to medium risk level because the *Serious* classification of the financial impact has changed toward one lower class, i.e. toward *Significant* classification. The risk mitigation from high to medium level is also verified in the green cluster of the feeder, between 18:00 and 22:00, when the financial impact decreases to *Significant* class. However, the assessed risk still remains at high level during the time period starting at 08:00 and ending 14:00 since the financial impact categories maintain the *Serious* and *Major* classification.

The aforementioned risk assessment has intense variation during the day as a consequence, in most cases, of the severe weather forecast. In days in which the forecasted meteorological parameters indicate calm weather, the variation of risk level is less intense. The cumulative risk representation aims to minimize the effect of monotonous risk assessment providing a tool capable of diagnosing the distribution system for periods of time exceeding one day. This property comes from the attribution of zero value to the low risk level, one to medium and two to the high-risk level. Figure 3 (a) shows a screenshot with heat map representation of cumulative risk level in one month to the base case where the cold color tones at the rear layers correspond to small accumulated risk while the warmer color tones at the front layers indicate the large accumulated risk. For comparison, Fig. 3 (b) displays the screenshot to the same feeder sections previously analyzed, but now the distribution network has automatic FLISR.

The red cluster of the feeder in the base case accumulates risk by covering the four rear layers. After the implementation of automatic FLISR, the accumulated risk does not grow up staying at the most rear layer, i.e. the purple layer. The drastic financial impact reduction to *Insignificant* classification and consequent monotonous incidences of the low risk level avoid the growth of the accumulated risk. Blue and green clusters of the feeder have larger cumulative risk than red cluster. As in the hourly risk assessment, there are a number of occurrences with financial impact classified as *Catastrophic*. In terms of progression through the layers and color tones, the accumulated risk magnitude is at maximum by covering all layers, until the hottest color tone, in the base case. On the other hand, this progression is not so excessive with the FLISR

(a) (b)

Fig. 3. Screenshots with heat map representation of cumulative risk during a month: (a) base case; and (b) distribution network with FLISR.

implementation, which reaches until the orange color tone. The decrease of cumulative risk progression results in the financial impact mitigation where the maximum impact classification changes from *Catastrophic* to *Major*.

Risk assessment results in Fig. 2 and 3 and their meanings expose the benefits of automatic FLISR implementation. There are feeder clusters where the risk mitigation is very intense while, in other clusters, the aggregated gain is not complete allowing for the incidence of high-risk level in a few hours of the day. The load balancing by DRM when distribution network is jeopardized also works as a potential risk mitigation technology that is analyzed in the next evaluation step.

The second step has the same features as the first evaluation step, in addition to the input parameters characterizing the responsive loads. The penetration percentages of responsive loads are 0.5, 0.3 and 0.1 for residential, commercial and industrial consumers, respectively, where the percentage of responsive load comes from general consumption patterns available in [24]. After the risk assessment characterization with input parameters, screenshots of the developed GIS visualization tool provide risk level behavior hour-by-hour. Figure 2 (c) displays a screen portion of the sunburst chart representation of risk levels hour-by-hour for the case of distribution network with FLISR in January, 14th of 2016. The improvements with the DRM implementation produce the hourly risk level variations, as is comparatively shown by the screenshot in Fig. 4 (a). Since the DR controller just receives the load shedding signal when the system is jeopardized, the red cluster of the feeder changes dramatically its risk level pattern during the day, from medium to low risk level. Similarly, blue and green clusters of the feeder change their patterns eliminating the incidence of the high-risk level. Most notable risk pattern change comes from green cluster of the feeder where the olive green replaces the dark red color in the time period between 08:00 and 14:00 hours that results from the financial impact reduction of *Major* and *Serious* classification to *Significant* classification. Lastly, the proposed risk assessment approach outputs the same risk pattern for blue and green clusters of the feeder.

In addition to hourly risk assessment under severe weather forecast, the monthly accumulated risk is evaluated in the case of the DRM implementation. Figure 3 (b) displays a screen portion with heat map representation of cumulative risk level in January of 2016 to the distribution network with FLISR. For comparison, Fig. 4 (b) shows the same screen portion after the DRM implementation in the test distribution network. The

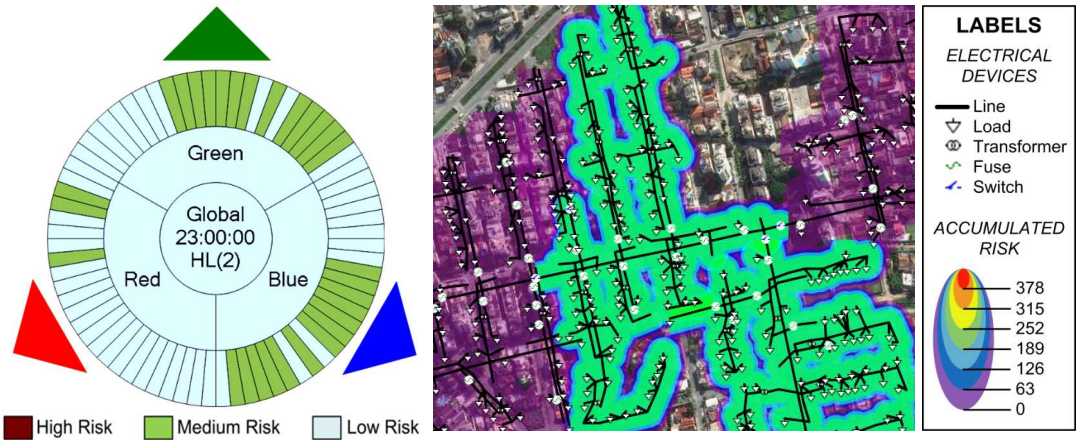

(a) (b)

Fig. 4. Screenshots of automated FLISR and DRM implementation: (a) hourly sunburst chart; and (b) heat map representation of cumulative risk.

red cluster of the feeder accumulates the same risk magnitude of the test distribution network with FLISR even after the DRM implementation repeating the behavior that is achieved in hourly risk assessment as previously commented. The decrease in the cumulative risk progression in blue and green clusters of the feeder is again verified. Before the DRM implementation, the cumulative risk progression reaches the orange layer. After the DRM, the progression only reaches the green layer. This decrease in the accumulated risk magnitude comes from financial impact reduction to *Significant* classification. At last, the cumulative risk progression in both blue and green clusters of the feeder have reached the same layer in graphical representation.

V. CONCLUSION

The study has made the following contributions:

- The online risk assessment framework to identify distribution network regions with different risk levels is applied in the evaluation of the self-healing technologies, such as automatic FLISR and DRM, for mitigating risk;
- The screenshots with sunburst chart representations of risk assessment hour-by-hour show benefits of the FLISR implementation through the change from medium to low and from high to the medium risk level in many feeder sections. The cumulative risk representation confirms the previous benefits showing sections without accumulated risk in the heat map as a consequence;
- In the case of DRM implementation, the risk assessment graphical representation from developed GIS visualization tool allows for identifying the suppression of high-risk level in the hourly assessment and the consequent decrease in accumulated risk magnitude in the monthly assessment;
- Both cases used for evaluation are examples of how the developed GIS visualization tool is able to represent clusters of the feeder in a dynamic sunburst chart and heat maps. The outcome reveals the benefits of risk-based decision-making framework on control and analysis of power distribution networks.

REFERENCES

[1] D. Vose, "Risk Analysis: A Quantitative Guide," vol. 1, 3rd ed., West Sussex, England: John Wiley & Sons, 2008, 729 pp.

[2] A. Monticelli, "State Estimation in Electric Power Systems: A Generalized Approach," illustrated ed., Springer, 1999.

[3] A. Abur and A. G. Expósito, "Power System State Estimation: Theory and Implementation," 1st ed., New York, NY, CRC Press, 2004.

[4] J. B. Leite, J. R. S. Mantovani, T. Dokic, Q. Yan, P. Chen and M. Kezunovic, "Resiliency Assessment in Distribution Networks using GIS Based Predictive Risk Analytics," *IEEE Trans. Power Syst.*, vol. 34, no. 6, pp. 4249-4257, Nov. 2019.

[5] J. B. Leite, J. R. S. Mantovani, T. Dokic, Q. Yan, P. Chen and M. Kezunovic, "The Impact of Time Series-Based Interruption Cost on Online Risk Assessment in Distribution Networks," *in Proc. 2016 IEEE PES Transmission and Distribution Conference and Exposition Latin America (T&D LA 2016)*, Morelia, Mexico, 2016, pp. 1-6.

[6] S. Borlase, "Smart Grid Technologies," in *Smart Grids: Infrastructure, Technology and Solutions*, 1st ed., vol. 1, Boca Raton: CRC Press, 2013, pp. 67-496.

[7] J. B. Leite and J. R. S. Mantovani, "Development of a Self-Healing Strategy with Multiagent Systems for Distribution Networks," *IEEE Trans. Smart Grid*, v. PP, pp. 1-9, Jan. 2016.

[8] M. Panteli and P. Mancarella, "Influence of extreme weather and climate change on the resilience of power systems: Impacts and possible mitigation strategies," *Elect. Power Syst. Res.*, vol. 127, pp. 259–270, Jun. 2015.

[9] M. Panteli and P. Mancarella, "The grid: stronger, bigger, smarter?: Presenting a conceptual framework of power system resilience*," IEEE Power and Energy Magazine*, vol. 13, no. 3, pp. 58–66, Apr. 2015.

[10] J. B. Leite, J. R. S. Mantovani, T. Dokic, Q. Yan, P. Chen and M. Kezunovic, "Failure probability metric by machine learning for online risk assessment in distribution network," in *Proc. 2017 IEEE PES Innovative Smart Grid Technologies Conference - Latin America (ISGT LA 2017)*, Quito, Ecuador, 2017, pp. 1-6.

[11] M. E. Paté-Cornell, "The Engineering Risk-Analysis Method and Some Applications," in *Advances in Decision Analysis from Foundations to Applications*, 1st ed., vol. 1, Cambridge University Press, 2012, pp. 302-324.

[12] C. Chen, J. Wang and D. Ton, "Modernizing Distribution System Restoration to Achieve Grid Resiliency Against Extreme Weather Events: An Integrated Solution," *Proc. IEEE*, vol. 105, no. 7, pp. 1267-1288, Jul. 2017.

[13] "Fault Location, Isolation and Service Restoration Technologies Reduces Outage Impact and Duration," *U. S. Department of Energy Office of Electricity Delivery and Energy Reliability*, Washington, DC, USA, 2014.

[14] J. R. Aguero, "Applying Self-Healing Schemes to Modern Distribution Systems," *2012 IEEE PES General Meeting*, San Diego, CA, 2012.

[15] R. Das, V. Madani, F. Aminifar, J. McDonald, S. S. Venkata, D. Novosel, A. Bose and M. Shahidehpour, "Distribution Automation Strategies: Evolution of Technologies and Business Case*," IEEE Trans. Smart Grid.*, vol. 6, no. 4, pp. 2166-2174, Jul. 2015.

[16] M. Eriksson, et. al, "Multiagent-Based Distribution Automation Solution for Self-Healing Grids," *IEEE Trans. Ind. Electron.*, vol. 62, no. 4, pp. 2620-2628, Apr. 2015.

[17] S. Borlase, "Smart Grid Barriers and Critical Success Factors," in *Smart Grids: Infrastructure, Technology and Solutions*, 1st ed., vol. 1, Boca Raton: CRC Press, 2013, pp. 497-530.

[18] B. Sivaneasan, K. N. Kumar, K. T. Tan and P. L. So, "Preemptive Demand Response Management for Buildings," *IEEE Trans. Sustain. Energy*, vol. 6, no. 2, Apr. 2015.

[19] "Assessment of demand response and advanced mitering," Federal. Energy Regulatory Commission. Report, Washington, DC, USA, 2010.

[20] H. Aki, "Demand-Side Resiliency and Electricity Continuity: Experiences and Lessons Learned in Japan," *Proc. IEEE*, vol. 105, no. 7, pp. 1443-1455, Jul. 2017.

[21] A. B. Lovins. "The Negawatt Revolution," *Across the Board*, vol. 27, no. 9, pp. 18-23, Sep. 1990.

[22] A. Safdarin, M. Lehtonen, M. Fotuhi-Firuzabad and R. Billinton, "Customer Interruption Cost in Smart Grids," *IEEE Trans. Power Syst.*, vol. 29, no. 2, pp. 994-995, Mar. 2014.

[23] R. Stamminger, "Synergy Potential of Smart Appliances," *EIE project: Smart Domestic Appliances in Sustainable Energy Systems*, D2.3 of WP 2 from the Smart-A project, Mar. 2009, pp. 220.

[24] Distribution testing system of 1807 lines, accessed: Mar. 03, 2016. [Online]. Available: http://www.feis.unesp.br/Home/departamentos/engenhariaeletrica/lapsee807/home/distribution_network_1806_lines.rar

[25] J. B. Leite, J. R. S. Mantovani, and M. Kezunovic, "Use of Distribution Network Topological Fractality and Sunburst Charts in the Online Risk Assessment," *Proc. 2019 IEEE PES Innovative Smart Grid Technologies Conference – Latin America (ISGT - LA 2019)*, Gramado, Brasil, 2019, pp. 1-6.